Report

Current Biology

Astrocytes Regulate Daily Rhythms in the Suprachiasmatic Nucleus and Behavior

Highlights

- Astrocytes, like neurons, are synchronous circadian oscillators in the SCN
- SCN astrocytes modulate daily rhythms in locomotor behavior and SCN physiology
- Loss of Bmal1 in SCN astrocytes lengthens period in SCN neurons and behavior
- The circadian period of the SCN and locomotion depends on astrocyte period

Authors

Chak Foon Tso, Tatiana Simon, Alison C. Greenlaw, Tanvi Puri, Michihiro Mieda, Erik D. Herzog

Correspondence

herzog@wustl.edu

In Brief

Tso et al. show that SCN astrocytes are synchronized circadian oscillators just like neurons. Either loss of rhythm or lengthened period in SCN astrocytes increases the period of daily rhythms in SCN neurons and in locomotor activity, demonstrating that astrocytes contribute to the determination of daily rhythms in physiology and behavior.

Tso et al., 2017, Current Biology *27*, 1–7
April 3, 2017
http://dx.doi.org/10.1016/j.cub.2017.02.037

CellPress

Please cite this article in press as: Tso et al., Astrocytes Regulate Daily Rhythms in the Suprachiasmatic Nucleus and Behavior, Current Biology (2017), http://dx.doi.org/10.1016/j.cub.2017.02.037

Current Biology
Report

Astrocytes Regulate Daily Rhythms in the Suprachiasmatic Nucleus and Behavior

Chak Foon Tso,[1] Tatiana Simon,[1] Alison C. Greenlaw,[1] Tanvi Puri,[1] Michihiro Mieda,[2] and Erik D. Herzog[1,3,*]
[1]Department of Biology, Washington University in St. Louis, St. Louis, MO 63108, USA
[2]Department of Molecular Neuroscience and Integrative Physiology, Kanazawa University, 920-1192 Ishikawa, Japan
[3]Lead Contact
*Correspondence: herzog@wustl.edu
http://dx.doi.org/10.1016/j.cub.2017.02.037

SUMMARY

Astrocytes are active partners in neural information processing [1, 2]. However, the roles of astrocytes in regulating behavior remain unclear [3, 4]. Because astrocytes have persistent circadian clock gene expression and ATP release in vitro [5–8], we hypothesized that they regulate daily rhythms in neurons and behavior. Here, we demonstrated that daily rhythms in astrocytes within the mammalian master circadian pacemaker, the suprachiasmatic nucleus (SCN), determine the period of wheel-running activity. Ablating the essential clock gene *Bmal1* specifically in SCN astrocytes lengthened the circadian period of clock gene expression in the SCN and in locomotor behavior. Similarly, excision of the short-period CK1ε *tau* mutation specifically from SCN astrocytes resulted in lengthened rhythms in the SCN and behavior. These results indicate that astrocytes within the SCN communicate to neurons to determine circadian rhythms in physiology and in rest activity.

RESULTS

Aldh1L1-Cre Reliably Labels Astrocytes within the SCN

We targeted astrocytes using Aldh1L1-Cre BAC transgenic mice [9, 10] because Aldh1L1 expression in the brain is high, broad, and specific to astrocytes [9]. To test the specificity and expression pattern of Aldh1L1 in the SCN, we crossed Aldh1L1-Cre/$^{+}$ mice to mice carrying Cre-activated nuclear GFP transgene (LSL-GFP^{NLS} [nucleus-localization signal]; Table S2 details the genotypes and treatments for all experiments). Immunofluorescence staining showed that Aldh1L1-GFP^{NLS} labels 10.9% ± 1.1% of SCN cells (n = 6 mice, one brain section each, mean ± SEM). The astrocyte marker glial fibrillary acidic protein (GFAP) labeled 96.4% ± 1.7% of the Aldh1L1-GFP^{NLS}-positive cells (Figure 1A; n = 1 section each from four mice). None of the Aldh1L1-GFP^{NLS} cells expressed the neuronal markers FOX2 (a homolog of NeuN [11, 12]; Figure 1B; n = 3 brains, 762 FOX2^{+} cells counted) or arginine vasopressin (AVP) (Figure S1; n = 6 brains, 220 AVP^{+} cells counted). In summary, the Aldh1L1-Cre mouse line provides one way to specifically label astrocytes in the SCN.

Astrocytes Function as Circadian Oscillators in the SCN

Previous work has shown that cortical astrocyte cultures and an astrocyte-like cell line (SCN2.2) have circadian rhythms in clock gene expression and release of ATP, a potent gliotransmitter [5–8]. To determine whether SCN astrocytes possess daily rhythms in clock genes, we stained Aldh1L1-GFP^{NLS} brain sections for BMAL1 (also called ARNTL or MOP3). We found that 85.9% ± 5.6% (n = 6 mice perfused at zeitgeber time [ZT] 2) of Aldh1L1 cells in the SCN expressed BMAL1 (Figure 1C). We next infected Aldh1L1-Cre/$^{+}$ organotypic SCN slices with a novel adeno-associated virus carrying a Cre-activated bioluminescent reporter of *Bmal1* transcription (AAV2/10-Bmal1ext-DIO-luc; Figure 2A). These Aldh1L1-Bmal1^{luc} SCN slices were rhythmic with a circadian period (23.6 ± 0.2 hr, n = 6; Figure 2C) and ~10-fold higher light emission than a Cre^{-} littermate SCN infected with the same virus (Table S1). For comparison, we found similar amplitude *Bmal1-luc* rhythms in SCN vasoactive intestinal polypeptide (VIP) neurons (Table S1). To measure coordination among SCN astrocytes, we imaged Aldh1L1-Bmal1^{luc} with an ultracooled charge-coupled device (CCD) camera (n = 3 SCN). We reliably detected astrocyte-shaped cells expressing the reporter of *Bmal1* activity throughout the SCN (Figure 2B; data not shown). Bioluminescence in 72.8% ± 4.0% of cell-sized regions of interest (ROIs) was circadian and peaked at a similar time each day (Figure 2D; $p < 0.0001$, Rayleigh's test, mean vector length = 0.85 ± 0.02). The remaining ROIs were considered arrhythmic. We conclude that astrocytes function as synchronous circadian oscillators within the SCN.

Loss of Daily Rhythms in SCN Astrocytes Lengthens Circadian Period in the SCN and in Behavior

Using a recently developed gene editing technique [13, 14], we ablated the *Bmal1* gene from targeted cells. In this strategy, short guide RNAs (sgRNAs) designed to direct the disruption of the *Bmal1* gene were delivered to cells expressing the CRISPR machinery under the control of cell-type-specific promoters. As a proof of concept, we injected a mixture of adeno-associated virus (AAV) carrying ubiquitously expressed pCBh-Cre and sgRNA against either LacZ (control, sgLacZ) or Bmal1 (sgBmal1; E1 and E3 denote independent sequences targeting exons 1 or 3 of the *Bmal1* gene) into the SCN of LSL-Cas9/$^{+}$; PER2::luc/$^{+}$ mice. We found that Cas9 was subsequently expressed throughout the SCN from a GFP fusion protein co-expressed with Cas9 (data not shown). Animals that received sgBmal1 lost daily rhythms in both behavior (n = 2 of 2 mice, one for each Bmal1 sgRNA vector) and whole SCN PER2::luc

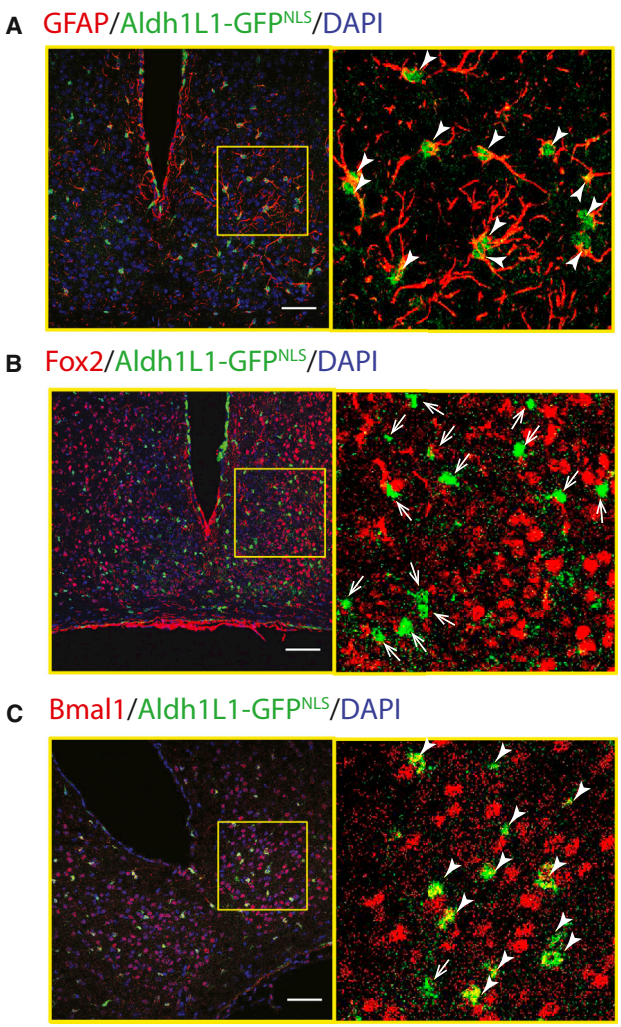

Figure 1. Astrocytes Targeted in the SCN with the Aldh1L1-Cre/$^{+}$ Mouse Line

Astrocyte nuclei in the SCN were labeled in green by Cre-mediated recombination of Aldh1L1-Cre/$^{+}$;LSL-GFP^{NLS}/$^{+}$ mice. Coronal brain sections were immunostained for an astroglial marker GFAP (A), a neuronal marker FOX2 (B), or a circadian clock protein BMAL1 (C) in red, and all nuclei were counterstained with DAPI. Cells within the yellow boxes (left) were magnified (right). Filled arrowheads indicate double-labeled cells, and arrows point to cells that showed no red and green colocalization. Note that Aldh1L1-positive cells reliably express the astrocyte marker GFAP and the circadian clock protein BMAL1, but not the neuronal marker FOX2. Scale bar, 75 μm. See also Figure S1.

(n = 12 of 12 SCN, n = 6 for each Bmal1 sgRNA vector) as predicted for global Bmal1 knockouts [15], while those that received sgLacZ (n = 2 of two mice and 5 of five SCN) remained circadian (Figure S2).

To test the necessity of astrocytes' molecular clocks in behavioral rhythms, we injected AAV carrying sgBmal1 into the SCN of Aldh1L1-Cre/$^{+}$; LSL-Cas9/$^{+}$ mice (Astro-Bmal1$^{-/-}$) and Cre^{-} littermate controls (Figure 3A). Before AAV injection, LSL-Cas9/$^{+}$ and Aldh1L1-Cre/$^{+}$; LSL-Cas9/$^{+}$ mice showed similar wheel-running periods in constant darkness (23.79 ± 0.05 hr, n = 9 and 23.75 ± 0.08 hr, n = 12, Student's t test, not significant [n.s.]). Strikingly, CRISPR-mediated loss of *Bmal1* in SCN astrocytes significantly lengthened their locomotor periodicity (Figures 3B and 3E; controls versus Aldh1L1-Bmal1$^{-/-}$: sgBmal1_E1: 23.76 ± 0.12 hr, n = 5 versus 24.22 ± 0.10 hr, n = 6; sgBmal1_E3: 23.75 ± 0.08 hr, n = 4 versus 24.38 ± 0.13 hr, n = 3; $p < 0.01$; one-way ANOVA with Sidak multiple comparison test). Loss of *Bmal1* in SCN astrocytes was confirmed by immunohistochemistry (Figures 3C and 3D; 2.5% ± 1.2% of cells were BMAL1- and Aldh1L1-positive cells, and nearly 97.7% ± 0.1% of Aldh1L1-Cas9 cells were GFAP positive; Bmal1: n = 9; GFAP: n = 6). In Aldh1L1-Bmal1$^{-/-}$ SCN, the period of *PER2::luc* rhythms was also significantly lengthened compared to Cre^{-} littermate controls (Figures 3F and 3G; 24.63 ± 0.14 hr, n = 6 versus 25.82 ± 0.41 hr, n = 5, $p < 0.05$, Student's t test). Using a CRISPR-independent approach, we again found period lengthening of circadian rhythms in flox Bmal1 mice injected with AAV8-GFAP-Cre-GFP compared to flox Bmal1 mice injected with a control AAV8-GFAP-GFP (23.7 ± 0.09 hr, n = 5 versus 23.07 ± 0.07 hr, n = 7; $p < 0.01$, t test). We conclude that loss of *Bmal1* in SCN astrocytes lengthens circadian rhythms in SCN neurons and behavior.

Circadian Period of SCN Astrocytes Regulates Circadian Period of the SCN and of Locomotor Behavior

Because BMAL1 is a transcription factor with circadian and non-circadian functions, we utilized the CK1ε *tau* mutation as an independent method to conditionally manipulate daily timing in astrocytes. This point mutation in exon 4 of the CK1ε gene shortens the period of wheel-running activity under constant darkness (*CK1ε*$^{tau/tau}$: ~20 hr, *CK1ε*$^{tau/+}$: ~22 hr) [16, 17]. The phenotype can be reversed when exon 4 is floxed out by Cre recombinase so that CK1ε$^{+/-}$ or CK1ε$^{-/-}$ mice have a 24-hr period [16]. We found that Cre^{-} littermates (termed *CK1ε*$^{tau/+}$) showed an ~22-hr period as previously reported, while *Aldh1L1-Cre/*$^{+}$*; CK1ε*$^{tau/+}$*; PER2::luc/*$^{+}$ (referred to as Aldh1L1- CK1ε$^{tau/+}$) animals showed a significantly lengthened period (Figures 4A and 4B; 22.21 ± 0.13 hr, n = 9 versus 23.42 ± 0.10 hr, n = 11, Student's t test, $p < 0.0001$). The SCN of Aldh1L1- CK1ε $^{tau/+}$ mice also showed lengthened PER2::luc rhythms (Figures 4C and 4D; 22.1 ± 0.18 hr versus 26.06 ± 0.68 hr, n = 5 SCN per group, Student's t test, $p < 0.01$), indicating the behavioral period directly results from the lengthened rhythm within the SCN.

We next infected CK1ε $^{tau/+}$ mice with a virus (AAV8-GFAP-Cre-GFP) to remove the *tau* mutation specifically in GFAP(+) astrocytes of the SCN (Figure 4E). Animals infected with the GFAP-Cre virus, like Aldh1L1- CK1ε$^{tau/+}$ mice, had a lengthened period in locomotor activity (Figures 4F and 4H; 22.54 ± 0.14 hr versus 23.43 ± 0.25 hr, n = 4 per group, Student's t test, $p < 0.05$) and in isolated SCN PER2::luc rhythms (Figures 4I–4J; 22.34 ± 0.12 hr versus 25.08 ± 0.41 hr, n = 4 per group, Student's t test, $p < 0.001$). AAV infection was confirmed by GFP fluorescence in the SCN (Figure 4G). Taken together, these results show that two independent methods that increased the period of SCN astrocytes relative to the rest of the body lengthened the periods of SCN and behavioral rhythms.

DISCUSSION

Here, four independent manipulations of clock genes in astrocytes similarly changed daily rhythms in the SCN and in behavior.

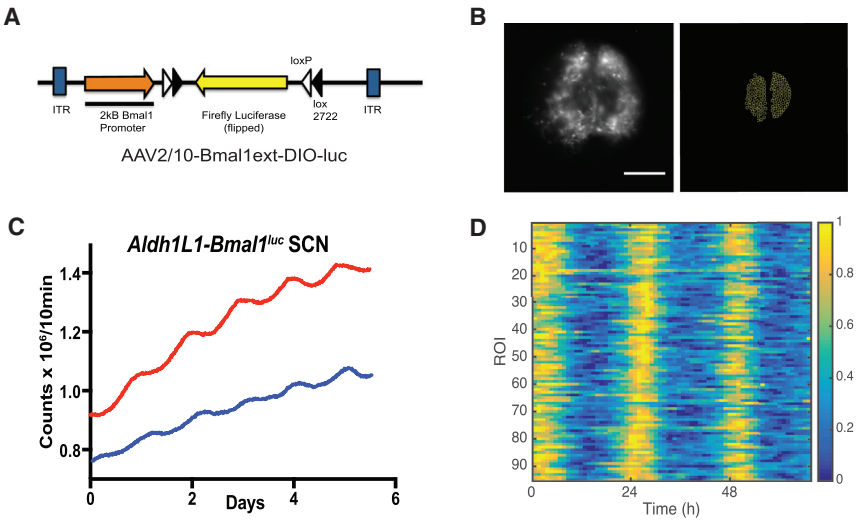

Figure 2. SCN Astrocytes Are Functional Circadian Oscillators

(A) Schematic of AAV-Bmal1ext-DIO-luc vector that provides a real-time, cell-type-specific report of *Bmal1* transcription.

(B) Left: representative frame from a movie of bioluminescence recorded from an Aldh1L1-Bmal1^{luc} SCN slice. Note the glowing astroglial cells throughout the bilateral SCN. Scale bar, 400 μm. Right: cell-sized regions of interest (ROIs) were used to track Bmal1 expression from astrocytes within the SCN.

(C) Representative bioluminescence traces from photomultiplier tube (PMT) recording of two Aldh1L1-Bmal1^{luc} SCN slices.

(D) Raster plot of Bmal1 reporter expression across a representative Aldh1L1-Bmal1^{luc} SCN slice from (B). The bioluminescence in each ROI peaked at approximately the same time daily over the 3 days of recording with an ultracooled CCD camera. Bioluminescence for each ROI was normalized to its maximum and pseudocolored (color bar at right). See also Table S1.

Although previous publications implicated astrocytes in SCN function (reviewed in [18, 19]), we lacked the tools to target these glial cells directly. Using promoters for GFAP and Aldh1L1 to drive reporters and manipulate clock genes, we were able to control astrocytes specifically within the SCN in vivo and in vitro. A conditional, real-time reporter of *Bmal1* transcription revealed synchronous circadian rhythms in astrocytes within SCN slice cultures. This is consistent with the reported rhythms in extracellular ATP attributed to astroglia in the isolated SCN [6, 7] but differs from a study that did not find daily cycles in Per1-luc expression in SCN astrocytes [20]. That report was based on an absence of immunohistochemical evidence for colocalization of GFAP and luciferase and may have been confounded by low or anti-phase levels of the two proteins. Furthermore, circadian rhythms have been reported in Per1-luc, PER2::luc, Bmal1-luc, and ATP release in cultured cortical astrocytes [5, 8] and in PER levels in *Drosophila* glial cells [21, 22]. We conclude that astrocytes are functional circadian oscillators within the SCN. It will be important to investigate phase differences between daily rhythms in SCN neurons and astrocytes and whether oscillations of SCN neuronal firing [23], neuropeptide release [24], or metabolic demand [25] are coupled to astrocyte rhythms.

In this study, we found evidence that circadian clocks in SCN astrocytes, like in SCN neurons, are modulators of daily rhythms in the SCN and behavior. Loss of rhythm in SCN astrocytes through *Bmal1* deletion resulted in lengthened circadian period of rest-activity rhythms. A similar 1-hr increase in period was recently reported for mice in which AVP neurons had *Bmal1* knocked out [26]. Thus, in contrast to the arrhythmicity produced by ablation of the clock in many SCN neurons [27, 28], *Bmal1* deletion in a small proportion of SCN cells appears to change the period of the SCN and behavior. Specifically, loss of rhythmicity in the 20% of SCN cells that express AVP or the 10% cells that express Aldh1L1 or GFAP suffices to lengthen SCN periodicity. This is consistent with the results of genetic chimera mice where the circadian phenotype scaled with the fraction of SCN cells homozygous for the dominant-negative form of CLOCK [29]. We conclude that astrocytes likely play as important a role as any neuronal cell class in circadian timekeeping in the SCN and behavior.

Are circadian rhythms in astrocytes sufficient or necessary for daily rhythms in the SCN or behavior? Several recent studies have found that Bmal1 deletion or PER2 overexpression in SCN neurons abolished circadian rhythms in locomotion [28, 30, 31]. We therefore posit that having a molecular clock in astrocytes is not sufficient to sustain behavioral rhythms. Our finding that mice remain circadian after loss of Bmal1 in astrocytes also argues against the necessity of an astrocyte circadian clock. However, increasing the intrinsic period of SCN astrocytes by deletion of CK1ε reliably lengthens behavioral period. This is a striking result because increasing period in a subpopulation of SCN neurons does not necessarily drive behavioral rhythms to longer periods. For example, using drivers that include SCN AVP neurons (AVP, neuromedin-S [NMS], or Scg2) to alter clock gene expression can increase locomotor period [27, 31, 32], but overexpression of Clock $^{\Delta 19}$ in SCN VIP neurons (~10% of SCN neurons) does not lengthen behavioral period [31]. Furthermore, manipulations that would be predicted to increase the cell-intrinsic period by at least 4 hr, even when targeted to 40% of SCN cells (e.g., with Drd1a), also tend to have smaller and less reliable effects on behavioral period [33]. Remarkably, we found that deletion of CK1ε in astrocytes, which has the cell-autonomous effect of increasing period by about 2 hr, sufficed to increase the behavioral period by about 1.5 hr. Thus, our data argue that clocks in SCN astrocytes likely play a more important role than some SCN neurons in determining behavioral periodicity.

Our findings also highlighted that glia in mammals and *Drosophila* may play fundamentally different roles in their circadian circuits. In contrast to our findings in SCN astrocytes, glial-specific knockdown of the essential clock gene, *Per*, did not change PER expression in neurons or locomotor activity rhythms in flies [21, 34]. Since PER expression was absent from glia cells in those flies, it is possible that clock-less

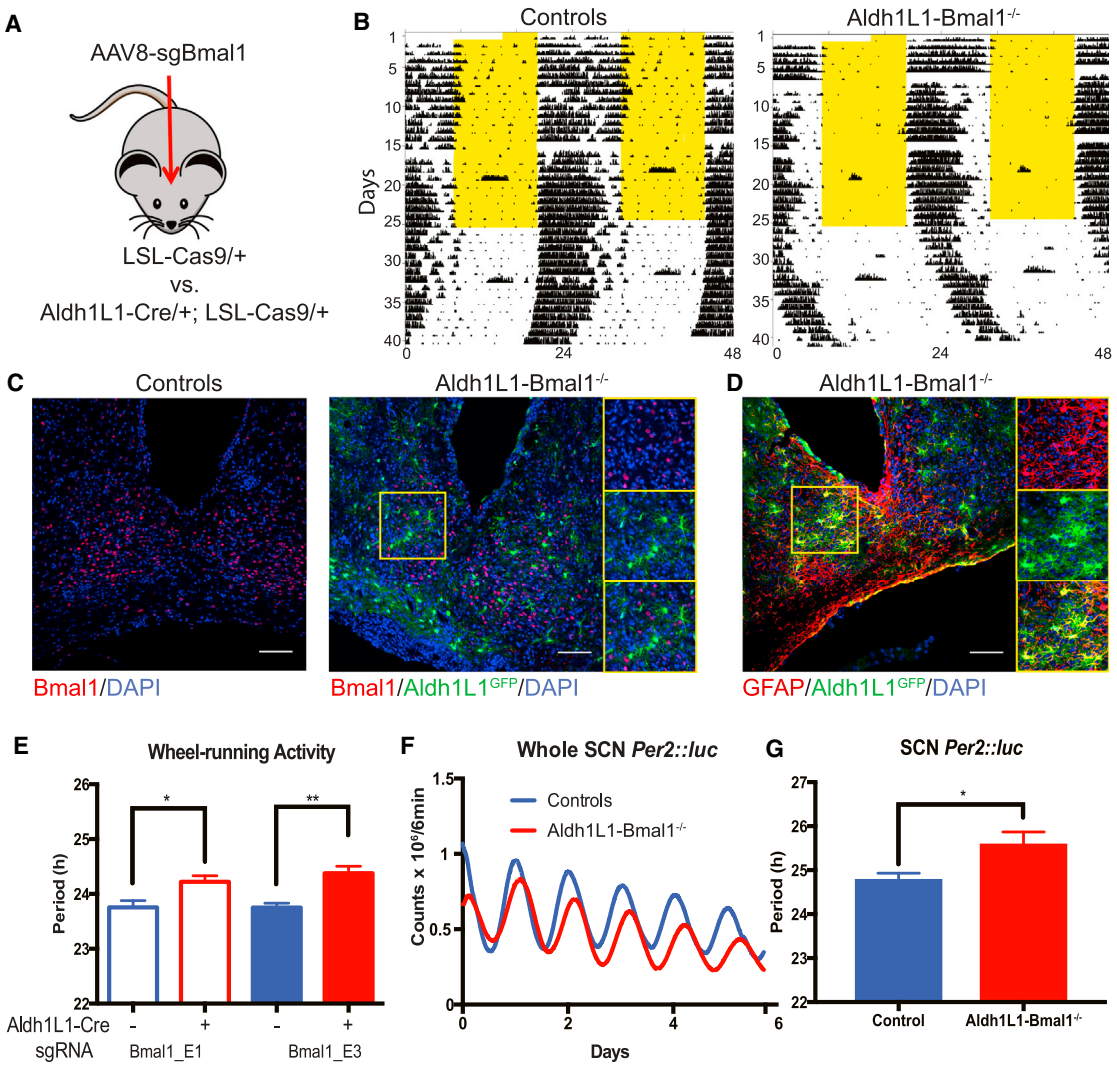

Figure 3. Loss of Bmal1 in SCN Astrocytes Lengthens Circadian Period In Vitro and In Vivo

(A) Schematic showing how CRISPR was used to delete the Bmal1 gene in SCN astroglia.

(B) Representative locomotor activity of a LSL-Cas9/$^{+}$ littermate control and an Aldh1L1-Cre/$^{+}$; LSL-Cas9/$^{+}$ mouse both injected with AAV-sgBmal1_E3 into bilateral SCN. Each line shows wheel running (black ticks) over 2 days with the second day's data replotted on the line below. The mice were less active in the light (yellow) in the 12-hr:12-hr light:dark cycle of the first 25 days of recording and showed free-running rhythms in constant darkness.

(C) Coronal brain sections immunostained for Bmal1 (red) and GFP (green) with insets showing the abundant BMAL1 staining in the control and lack of BMAL1 in Aldh1L1 cells in mouse with targeted deletion.

(D) GFAP staining (red) reliably colocalized with Cre-activated GFP (green) in this representative SCN of an Aldh1L1-Cas9 mouse.

(E) *Bmal1* ablation in Aldh1L1 cells by either of two independent guide RNAs (E1 or E3) in the SCN increased the circadian period of locomotor activity compared to Cre^{-} controls. *$p < 0.05$; **$p < 0.01$, one-way ANOVA with Sidak multiple comparison test.

(F) Representative PER2::luc traces from the cultured SCN of a Aldh1L1-Cre/$^{+}$; LSL-Cas9/$^{+}$; PER2::luc/$^{+}$ mouse (red) and a LSL-Cas9/$^{+}$; PER2::luc/$^{+}$ littermate control (blue) both injected with sgBmal1_E3 into bilateral SCN in vivo.

(G) Loss of Bmal1 lengthened circadian period in the isolated SCN. *$p < 0.05$; t test. Scale bars, 75 μm. Error bars, mean ± SEM.

See also Figure S2.

astrocytes in the fly brain can be driven to oscillate by circadian neurons so that behavior remains intact. Alternatively, it may be that loss of PER in flies is not equivalent to loss of Bmal1 in mice. The consequence of the loss of the Bmal1 ortholog, Cyc, is yet to be tested in glial cells in flies. Notably, in flies, loss-of-function mutation in the glial-specific, clock-controlled gene *ebony* [35] or glial-specific perturbations of membrane potential, vesicular release, or intracellular Ca^{2+} storage can lead to behavioral arrhythmicity. This suggests that dysregulation of glial physiology can interfere with daily rhythms in physiology and behavior in flies. Future studies should test whether and which cellular functions of SCN astrocytes are necessary for rhythmicity in the SCN and behavior.

Since our experiments ablating BMAL1 or rescuing the *tau* mutation in SCN astrocytes all resulted in a remarkably similar period lengthening in vitro and in vivo, it is likely that any genetic

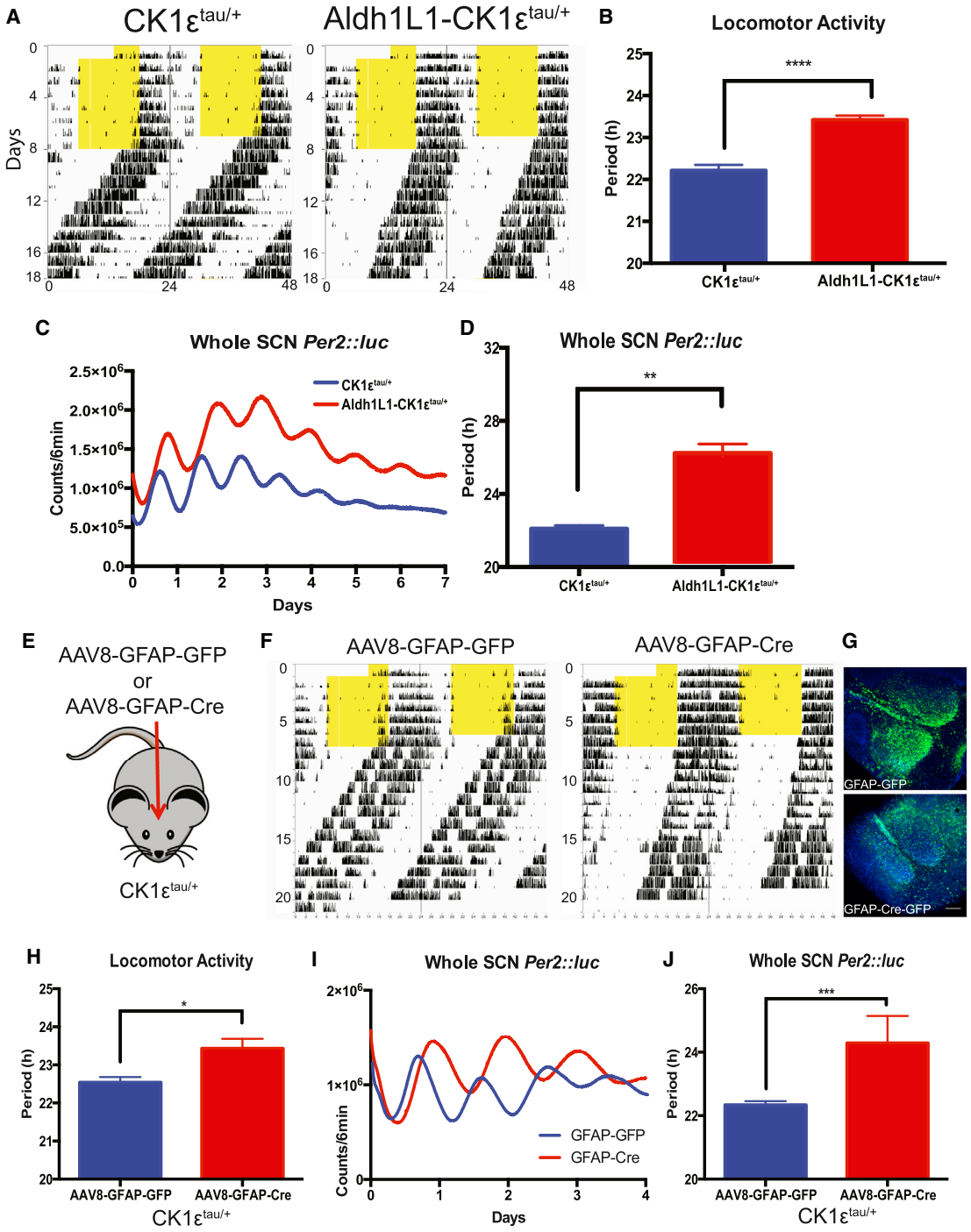

Figure 4. Loss of CK1ε in SCN Astrocytes Lengthens Circadian Period In Vivo and In Vitro

(A and B) Representative actograms of Aldh1L1- CK1$\varepsilon^{tau/+}$ and CK1$\varepsilon^{tau/+}$ littermates (A) showing how locomotor activity free-ran in constant darkness with a longer circadian period in mice where the CK1$\varepsilon^{tau/+}$ mutation was removed from astrocytes (B) ($p < 0.0001$, t test).

(C and D) Representative PER2::luc recordings from the isolated SCN of Aldh1L1- CK1$\varepsilon^{tau/+}$ and CK1$\varepsilon^{tau/+}$ littermates (C) with a longer circadian period in SCN where the CK1$\varepsilon^{tau/+}$ mutation was removed from astrocytes (D) ($p < 0.01$, t test).

(E) Schematic of a second method to change circadian timing in astrocytes using GFAP AAV injection to CK1$\varepsilon^{tau/+}$ SCN in vivo.

(F and G) Representative actograms of two CK1$\varepsilon^{tau/+}$ mice injected with either AAV8-GFAP-GFP or AAV8-GFAP-Cre-GFP (F) with successful viral targeting to the SCN (G).

(H) The circadian period of locomotor activity of AAV8-GFAP-Cre injected CK1$\varepsilon^{tau/+}$ mice was approximately 1 hr longer than controls ($p < 0.05$, t test).

(I) Representative whole SCN PER2::luc recording from CK1$\varepsilon^{tau/+}$ animals injected with either AAV8-GFAP-GFP or AAV8-GFAP-Cre-GFP.

(J) Period of PER2::luc recordings from AAV8-GFAP-Cre; CK1$\varepsilon^{tau/+}$ SCN was approximately 2 hr longer than controls ($p < 0.001$, t test). Error bars, mean ± SEM.

or environmental disruptions of daily rhythms in astroglia will alter daily rhythms in behavior. That is, it is unlikely that the period lengthening phenotype reflects functions of BMAL1 and CK1ε outside of circadian rhythms. This is supported by our prediction and finding that removal of the CK1ε *tau* mutation from SCN astrocytes would lengthen the period close to 24 hr. Thus, our data strongly argue that the astrocyte circadian clock regulates daily behaviors.

Why do genetic manipulations predicted to abolish or increase period in SCN astrocytes both result in a similar long period in the SCN and behavior? It could be that loss of BMAL1 or CK1ε similarly impacts a signal (or signals) from astrocytes (e.g., a diffusible factor, structural change, or a metabolic precursor) that influences daily rhythms in SCN neurons. Based on our data, this signal is not normally necessary for rhythmicity in neurons, but its levels are likely clock controlled and accelerate the period of the neuronal clock either directly or by modulating neuron-neuron interactions. Several testable predictions can be made with this proposed model: (1) arrhythmicity in astrocytes caused by disruption of either the positive (e.g., BMAL1 or CLOCK) or negative limb (e.g., PERs or CRYs) of the circadian transcription-translation feedback loop will always lengthen period; (2) combining SCN astrocytes with intrinsically different circadian periods with wild-type (WT) neurons will draw behavioral period toward the astrocyte period; (3) blocking signaling from SCN neurons to astrocytes will alter daily behavior and the phase relationship between rhythms in SCN neurons and astrocytes and/or between SCN neurons.

In summary, we found that SCN astrocytes have persistent daily rhythms in gene expression that modulate the period of SCN and rest-activity rhythms. These daily rhythms intrinsic to astrocytes may also contribute to other behaviors including sleep [4, 36].

EXPERIMENTAL PROCEDURES

Animals

Mice were housed in 12-hr:12-hr light:dark cycle with ad libitum food and water unless otherwise stated. Transgenic mice used here were Aldh1L1-Cre/$^{+}$ (Jax: 023748, founders were a gift from D. Rowitch, HHMI/UCSF), LSL-Cas9-eGFP (Jax: 024858), LSL-GFP^{NLS} (Jax: 008516), *CK1ε$^{tau/tau}$* (gift from M. Butler, OSHU [16]), VIP-IRES-Cre (Jax: 010908), Bmal1f/f (Jax: 007668), and PER2::luc (gift from J. Takahashi, HHMI/UT Southwestern). All procedures were approved by the Animal Care and Use Committee of Washington University and conformed to US National Institutes of Health guidelines.

Viral Vectors

We produced viruses carrying cell-type-specific Cre drivers or guide RNAs to delete Bmal1 in targeted cells. The pCBh-Cre construct was modified from AAV:ITR-U6-sgRNA(backbone)-pCBh-Cre-WPRE-hGHpA-ITR (Feng Zhang, Harvard, purchased from Addgene) by replacing the Cre sequence with mCherry-NLS from pcDNA3.1-Peredox plasmid (Gary Yellen, Harvard) to facilitate tracking of the virus (hereafter referred as sgBB). The following DNA sequences were inserted at the designated site of the sgRNA scaffold of sgBB:

AAV:ITR-U6-sgLacZ-pCBh-mCherry- NLS-WPRE-hGHpA-ITR
Sense sgRNA Sequence: 5′-TGCGAATACGCCCACGCGAT
AAV:ITR-U6-sgBmal1_E1-pCBh- mCherry-NLS-WPRE-hGHpA-ITR
Sense sgRNA Sequence: 5′-GTGTGGACTGCAATCGCAAG
AAV:ITR-U6-sgBmal1_E3_pCBh- mCherry-NLS-WPRE-hGHpA-ITR
Sense sgRNA Sequence: 5′-GTAGATAAACTCACCGTGCTA

All experimental sgRNAs had a score ≥ 89 from the CRISPR design tool (http://crispr.mit.edu/) with no apparent off-target sites and were designed to target genomic DNA sequences 5′ of bHLH and PAS domains of the Bmal1 gene. AAV2/8 sgRNA and pCBh-Cre vectors were generated by Hope Center Viral Vector Core at Washington University.

AAV2/10 Bmal1-DIO-luc was made by replacing Bmal1 cDNA in AAV2/10-Bmal1-DIO-Bmal1 [26] and generated by the Hope Center Viral Vector Core. AAV8-GFAP-GFP and AAV8-GFAP-Cre-GFP were from University of North Carolina Viral Vector Core.

AAV Infection

We injected viruses (0.4 μL/side) into the bilateral SCN in vivo (coordinates [in millimeters] from Bregma: anterior/posterior [A/P] 0 medial/lateral [M/L] ± 0.2 dorsal/ventral [D/V] −5.6) using a Hamilton Neuros Syringe. It should be noted that under this injection protocol some mCherry-NLS expression from the sgBmal1 AAV (Figure 3) was observed in neighboring hypothalamic areas along the third ventricle. Therefore, we cannot rule out loss of Bmal1 in some extra-SCN astrocytes. However, in the independent experiment using GFAP-Cre-GFP or GFAP-GFP AAVs, GFP expression was largely restricted to SCN (e.g., Figure 4G), indicating that changes to circadian timing in SCN astrocytes suffices to produce a circadian phenotype. We also infected P5-P6 SCN slices (250-μm coronal) after 2 days in vitro with 1 μL of AAV added directly on top of the SCN slice (Figure 2). The mice and the slices were allowed at least 2 weeks for recovery and viral expression prior to data collection.

SUPPLEMENTAL INFORMATION

Supplemental Information includes two figures, two tables, and Supplemental Experimental Procedures and can be found with this article online at http://dx.doi.org/10.1016/j.cub.2017.02.037.

AUTHOR CONTRIBUTIONS

C.F.T. and E.D.H. designed research. C.F.T., T.S., A.C.G., and T.P. performed research. C.F.T., A.C.G., T.P., and E.D.H. analyzed data. C.F.T. and E.D.H. wrote the manuscript. AAV2/10-Bmal1-DIO-luc is an unpublished reagent generated by M.M.

ACKNOWLEDGMENTS

We thank Dr. Andrew Liu for providing the *Bmal1:luc* NIH 3T3 cell line that was used in the preliminary testing of the sgRNA constructs. We thank Drs. Erik Musiek and Hal Gainer for sharing antibodies. We thank Herzog lab members for discussions and S. Allu for assistance in data analysis. Bmal1 sgRNA AAV vectors were generated by the Hope Center Viral Vector Core with support from a Hope Center Just-in-Time Grant. This work is supported by NIBIB grant 21956 and NINDS grant 095367.

Received: January 2, 2017
Revised: February 9, 2017
Accepted: February 15, 2017
Published: March 23, 2017

REFERENCES

1. Chung, W.S., Welsh, C.A., Barres, B.A., and Stevens, B. (2015). Do glia drive synaptic and cognitive impairment in disease? Nat. Neurosci. *18*, 1539–1545.
2. Zuchero, J.B., and Barres, B.A. (2015). Glia in mammalian development and disease. Development *142*, 3805–3809.
3. Bazargani, N., and Attwell, D. (2016). Astrocyte calcium signaling: The third wave. Nat. Neurosci. *19*, 182–189.
4. Haydon, P.G., and Nedergaard, M. (2014). How do astrocytes participate in neural plasticity? Cold Spring Harb. Perspect. Biol. *7*, a020438.
5. Marpegan, L., Swanstrom, A.E., Chung, K., Simon, T., Haydon, P.G., Khan, S.K., Liu, A.C., Herzog, E.D., and Beaulé, C. (2011). Circadian regulation of ATP release in astrocytes. J. Neurosci. *31*, 8342–8350.
6. Burkeen, J.F., Womac, A.D., Earnest, D.J., and Zoran, M.J. (2011). Mitochondrial calcium signaling mediates rhythmic extracellular ATP

accumulation in suprachiasmatic nucleus astrocytes. J. Neurosci. *31*, 8432–8440.

7. Womac, A.D., Burkeen, J.F., Neuendorff, N., Earnest, D.J., and Zoran, M.J. (2009). Circadian rhythms of extracellular ATP accumulation in suprachiasmatic nucleus cells and cultured astrocytes. Eur. J. Neurosci. *30*, 869–876.
8. Prolo, L.M., Takahashi, J.S., and Herzog, E.D. (2005). Circadian rhythm generation and entrainment in astrocytes. J. Neurosci. *25*, 404–408.
9. Cahoy, J.D., Emery, B., Kaushal, A., Foo, L.C., Zamanian, J.L., Christopherson, K.S., Xing, Y., Lubischer, J.L., Krieg, P.A., Krupenko, S.A., et al. (2008). A transcriptome database for astrocytes, neurons, and oligodendrocytes: A new resource for understanding brain development and function. J. Neurosci. *28*, 264–278.
10. Molofsky, A.V., Kelley, K.W., Tsai, H.H., Redmond, S.A., Chang, S.M., Madireddy, L., Chan, J.R., Baranzini, S.E., Ullian, E.M., and Rowitch, D.H. (2014). Astrocyte-encoded positional cues maintain sensorimotor circuit integrity. Nature *509*, 189–194.
11. Underwood, J.G., Boutz, P.L., Dougherty, J.D., Stoilov, P., and Black, D.L. (2005). Homologues of the Caenorhabditis elegans Fox-1 protein are neuronal splicing regulators in mammals. Mol. Cell. Biol. *25*, 10005–10016.
12. Kim, K.K., Adelstein, R.S., and Kawamoto, S. (2009). Identification of neuronal nuclei (NeuN) as Fox-3, a new member of the Fox-1 gene family of splicing factors. J. Biol. Chem. *284*, 31052–31061.
13. Platt, R.J., Chen, S., Zhou, Y., Yim, M.J., Swiech, L., Kempton, H.R., Dahlman, J.E., Parnas, O., Eisenhaure, T.M., Jovanovic, M., et al. (2014). CRISPR-Cas9 knockin mice for genome editing and cancer modeling. Cell *159*, 440–455.
14. Swiech, L., Heidenreich, M., Banerjee, A., Habib, N., Li, Y., Trombetta, J., Sur, M., and Zhang, F. (2015). In vivo interrogation of gene function in the mammalian brain using CRISPR-Cas9. Nat. Biotechnol. *33*, 102–106.
15. Bunger, M.K., Wilsbacher, L.D., Moran, S.M., Clendenin, C., Radcliffe, L.A., Hogenesch, J.B., Simon, M.C., Takahashi, J.S., and Bradfield, C.A. (2000). Mop3 is an essential component of the master circadian pacemaker in mammals. Cell *103*, 1009–1017.
16. Meng, Q.J., Logunova, L., Maywood, E.S., Gallego, M., Lebiecki, J., Brown, T.M., Sládek, M., Semikhodskii, A.S., Glossop, N.R., Piggins, H.D., et al. (2008). Setting clock speed in mammals: The CK1 epsilon tau mutation in mice accelerates circadian pacemakers by selectively destabilizing PERIOD proteins. Neuron *58*, 78–88.
17. Ralph, M.R., and Menaker, M. (1988). A mutation of the circadian system in golden hamsters. Science *241*, 1225–1227.
18. Evans, J.A. (2016). Collective timekeeping among cells of the master circadian clock. J. Endocrinol. *230*, R27–R49.
19. Jackson, F.R. (2011). Glial cell modulation of circadian rhythms. Glia *59*, 1341–1350.
20. Yamaguchi, S., Isejima, H., Matsuo, T., Okura, R., Yagita, K., Kobayashi, M., and Okamura, H. (2003). Synchronization of cellular clocks in the suprachiasmatic nucleus. Science *302*, 1408–1412.
21. Ng, F.S., Tangredi, M.M., and Jackson, F.R. (2011). Glial cells physiologically modulate clock neurons and circadian behavior in a calcium-dependent manner. Curr. Biol. *21*, 625–634.
22. Zerr, D.M., Hall, J.C., Rosbash, M., and Siwicki, K.K. (1990). Circadian fluctuations of period protein immunoreactivity in the CNS and the visual system of Drosophila. J. Neurosci. *10*, 2749–2762.
23. Inouye, S.T., and Kawamura, H. (1979). Persistence of circadian rhythmicity in a mammalian hypothalamic "island" containing the suprachiasmatic nucleus. Proc. Natl. Acad. Sci. USA *76*, 5962–5966.
24. Jin, X., Shearman, L.P., Weaver, D.R., Zylka, M.J., de Vries, G.J., and Reppert, S.M. (1999). A molecular mechanism regulating rhythmic output from the suprachiasmatic circadian clock. Cell *96*, 57–68.
25. Schwartz, W.J., and Gainer, H. (1977). Suprachiasmatic nucleus: Use of 14C-labeled deoxyglucose uptake as a functional marker. Science *197*, 1089–1091.
26. Mieda, M., Ono, D., Hasegawa, E., Okamoto, H., Honma, K., Honma, S., and Sakurai, T. (2015). Cellular clocks in AVP neurons of the SCN are critical for interneuronal coupling regulating circadian behavior rhythm. Neuron *85*, 1103–1116.
27. Hong, H.K., Chong, J.L., Song, W., Song, E.J., Jyawook, A.A., Schook, A.C., Ko, C.H., and Takahashi, J.S. (2007). Inducible and reversible Clock gene expression in brain using the tTA system for the study of circadian behavior. PLoS Genet. *3*, e33.
28. Izumo, M., Pejchal, M., Schook, A.C., Lange, R.P., Walisser, J.A., Sato, T.R., Wang, X., Bradfield, C.A., and Takahashi, J.S. (2014). Differential effects of light and feeding on circadian organization of peripheral clocks in a forebrain Bmal1 mutant. eLife *3*, 3.
29. Low-Zeddies, S.S., and Takahashi, J.S. (2001). Chimera analysis of the Clock mutation in mice shows that complex cellular integration determines circadian behavior. Cell *105*, 25–42.
30. Chen, R., Schirmer, A., Lee, Y., Lee, H., Kumar, V., Yoo, S.H., Takahashi, J.S., and Lee, C. (2009). Rhythmic PER abundance defines a critical nodal point for negative feedback within the circadian clock mechanism. Mol. Cell *36*, 417–430.
31. Lee, I.T., Chang, A.S., Manandhar, M., Shan, Y., Fan, J., Izumo, M., Ikeda, Y., Motoike, T., Dixon, S., Seinfeld, J.E., et al. (2015). Neuromedin s-producing neurons act as essential pacemakers in the suprachiasmatic nucleus to couple clock neurons and dictate circadian rhythms. Neuron *85*, 1086–1102.
32. Mieda, M., Okamoto, H., and Sakurai, T. (2016). Manipulating the cellular circadian period of arginine vasopressin neurons alters the behavioral circadian period. Curr. Biol. *26*, 2535–2542.
33. Smyllie, N.J., Chesham, J.E., Hamnett, R., Maywood, E.S., and Hastings, M.H. (2016). Temporally chimeric mice reveal flexibility of circadian period-setting in the suprachiasmatic nucleus. Proc. Natl. Acad. Sci. USA *113*, 3657–3662.
34. Jackson, F.R., Ng, F.S., Sengupta, S., You, S., and Huang, Y. (2015). Glial cell regulation of rhythmic behavior. Methods Enzymol. *552*, 45–73.
35. Suh, J., and Jackson, F.R. (2007). Drosophila ebony activity is required in glia for the circadian regulation of locomotor activity. Neuron *55*, 435–447.
36. Oliveira, J.F., Sardinha, V.M., Guerra-Gomes, S., Araque, A., and Sousa, N. (2015). Do stars govern our actions? Astrocyte involvement in rodent behavior. Trends Neurosci. *38*, 535–549.

Note Added in Proof

Two relevant papers were published while this study was in press. Barca-Mayo et al. found that loss of Bmal1 in astrocytes throughout the brain alters daily rhythms in locomotor activity, consistent with the SCN-specific results reported here. Brancaccio et al. demonstrated that removal of the homozygous tau (*Ck1ε*) mutation in astrocytes sufficed to increase period in behavior, consistent with the effects of removal of the heterozygous tau mutation reported here.

Barca-Mayo, O., Pons-Espinal, M., Follert, P., Armirotti, A., Berdondini, L., and De Pietri Tonelli, D. (2017). Astrocyte deletion of *Bmal1* alters daily locomotor activity and cognitive functions via GABA signalling. Nat. Commun. *8*, 14336.

Brancaccio, M., Patton, A.P., Chesham, J.E., Maywood, E.S., and Hastings, M.H. (2017). Astrocytes control circadian timekeeping in the suprachiasmatic nucleus via glutamatergic signaling. Neuron. Published online March 9, 2017. http://dx.doi.org/10.1016/j.neuron.2017.02.030.

Current Biology, Volume *27*

Supplemental Information

Astrocytes Regulate Daily Rhythms in the Suprachiasmatic Nucleus and Behavior

Chak Foon Tso, Tatiana Simon, Alison C. Greenlaw, Tanvi Puri, Michihiro Mieda, and Erik D. Herzog

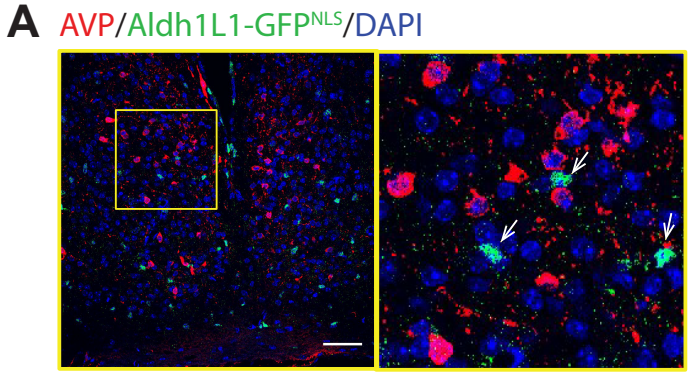

Figure S1. Aldh1L1-GFP^{NLS} does not label SCN neurons. Related to Figure 1.
(A) Astrocyte nuclei in the SCN were labeled (green) by Cre-mediated recombination of Aldh1L1-Cre/+;LSL-GFP^{NLS}/+ mice and then coronal brain sections were immunostained for AVP (red). The locations of the magnified images are indicated by yellow squares in the low-power images. Arrowheads illustrate that none of the Aldh1L1-positive cells labeled for AVP. Scale bar = 75 μm.

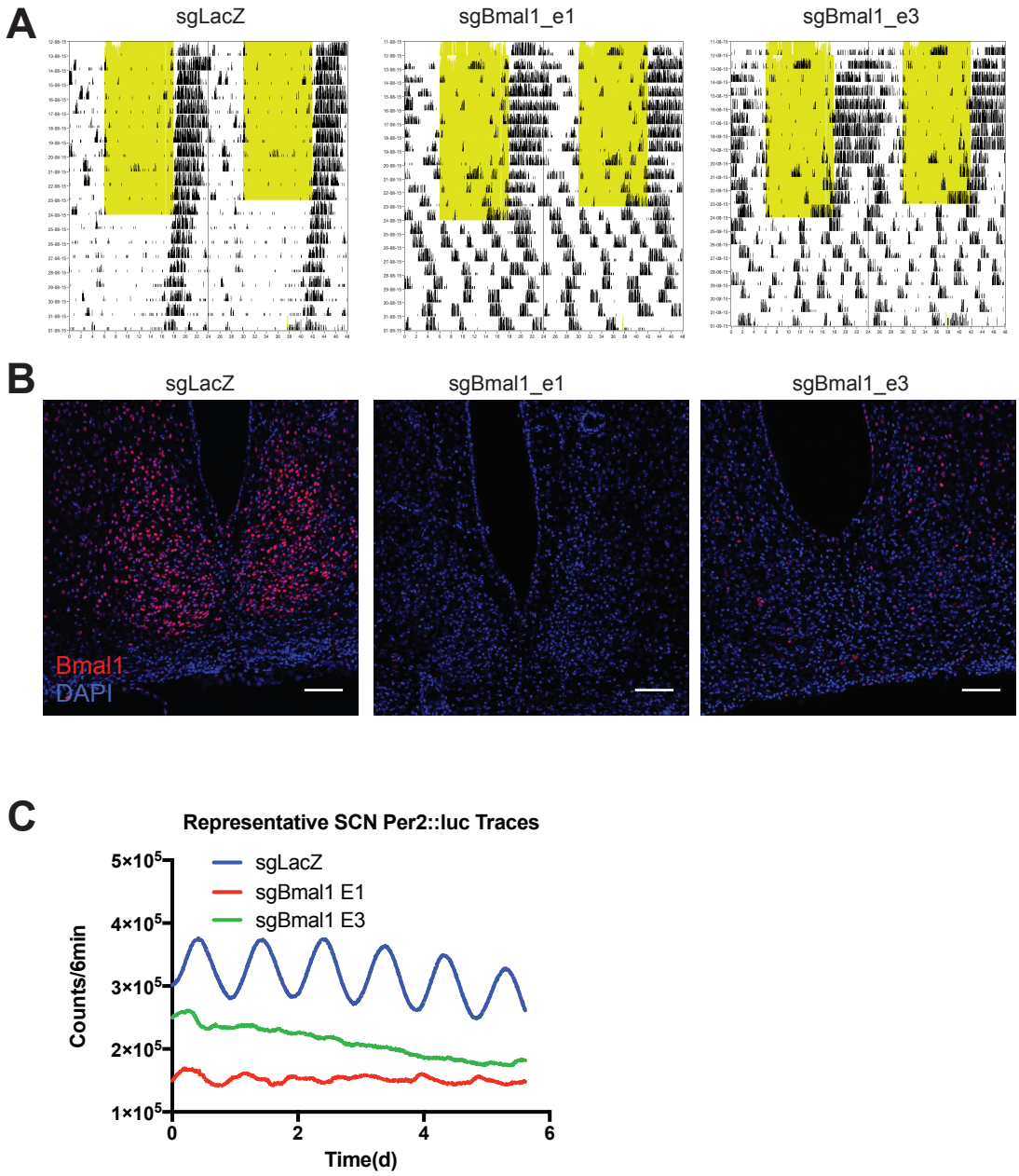

Figure S2. Loss of Bmal1 from all SCN cells phenocopies the global Bmal1 knockout. Related to Figure 3. (A) Representative actograms of LSL-Cas9/+; PER2::luc/+ animals which were injected with AAV carrying pCBh-Cre and either sgRNA against LacZ or Bmal1 (exon 1 or exon3) to the SCN. (B) BMAL1 staining (red) in the SCN of the animals shown in (A). (C) Representative PER2::luc traces from SCN slices which were infected with AAV carrying pCBh-Cre and either sgRNA against LacZ or Bmal1 (exon 1 [E1] or exon3[E3]). Note the arrhythmic PER2 expression in the two SCN where BMAL1-deletion was targeted to all cells and the circadian rhythm in the control.

Table S1: Summary statistics on AAV2/10-Bmal1ext-DIO-luc experiments. Related to Figure 2.

Genotype	Virus Added	Period	Amplitude ****	Goodness of Fit ***	Mean Bioluminescence (Counts/10min)*
Aldh1L1-Cre/+ (n = 6 mice)	AAV2/10-Bmal1ext-DIO-luc	23.6 ± 0.2 h	0.014 ± 0.002*	0.97 ± 0.007***	1,645,662 ± 578,301*
VIP-IRES-Cre (n = 4 mice)	AAV2/10-Bmal1ext-DIO-luc	23.1 ± 0.7 h	0.014 ± 0.003*	0.93 ± 0.03**	211,203 ± 13,778
WT (n = 2 mice)	AAV2/10-Bmal1ext-DIO-luc + AAV2/8-pCBh-Cre (1:1)	22.6 ± 0.1 h	0.033± 0.004****	0.98 ± 0.003**	178,785 ± 6,359
WT (n = 7 mice)	AAV2/10-Bmal1ext-DIO-luc	N.A.	0.006 ± 0.002	0.60 ± 0.07	92,647 ± 11,855

Statistics: One-way ANOVA with Bonferroni's multiple comparison test compared to no Cre control (underlined). *: $p< 0.05$; **: $p<0.01$; ***: $p< 0.001$; ****: $p<0.0001$.

Table S2. Detailed descriptions of the genetic manipulations in each figure. Related to all figures.

Glossary
Cre: Cre recombinase
Cas9: CRISPR-associated protein 9
DIO: double-floxed inverted orientation. Activated by Cre.
GFP: Green fluorescence protein
LSL: loxP-STOP-loxP. Activated by Cre
Luc: firefly luciferase
NLS: nuclear-localization signal
Rosa26: A mouse genomic locus commonly used for constitutive, ubiquitous expression.
sgBmal1_E1: sgRNA targeting exon 1 of *Bmal1*
sgBmal1_E3: sgRNA targeting exon 3 of *Bmal1*

All injections targeted the bilateral SCN.

Treatment	Full genotype	Description of genotype	Virus Injected	Description of Virus
Fig. 1 and S1				
Aldh1L1-GFP^{NLS}	Aldh1L1-Cre/+; LSL-GFP^{NLS}/+	Rosa26 knockin of LSL-GFP^{NLS} driven by ubiquitous promoter. Expression of nuclear-localized GFP was activated by Cre recombinase in Aldh1L1 (+) cells.	None.	None.
Figure 2 and Table S2				
Aldh1L1-$Bmal1^{luc}$	Aldh1L1-Cre/+	Cre recombinase was expressed in Aldh1L1 (+) cells.	AAV2/10-Bmal1ext-DIO-luc	$Bmal1^{luc}$ was activated only in Aldh1L1 (+) cells.
VIP-$Bmal1^{luc}$	VIP-IRES-Cre	Cre recombinase was expressed in vasoactive intestinal polypeptide (+) neurons.	AAV2/10-Bmal1ext-DIO-luc	$Bmal1^{luc}$ was activated only in VIP (+) neurons.
Positive Control	WT (No Cre)	WT mice.	AAV2/10-Bmal1ext-DIO-luc +	$Bmal1^{luc}$ was activated ubiquitously.

			AAV8-pCBh-Cre	
Negative Control	WT (No Cre)	WT mice.	AAV2/10-Bmal1ext-DIO-luc	Negative control to determine background bioluminescence.
Fig. 3				
Controls	LSL-Cas9-GFP/+; PER2::luc/+	Rosa26 knockin of LSL-Cas9-GFP driven by a ubiquitous promoter. Since Cre was absent, neither Cas9 nor GFP were expressed. PER2::luc was expressed in all cells.	AAV2/8-U6-sgBmal1-pCBh-mCherry^{NLS} (E1 or E3)	Ubiquitous expression of mCherry-NLS to report virus spread. In the presence of Cas9, a cut at the desired locus within the *Bmal1* gene was made. Non-homologous end joining (NHEJ) of DNA led to a frame shift and premature stop codon in the Bmal1 gene in most Cas9-expressing cells.
Aldh1L1-Bmal1-/-	Aldh1L1/+; LSL-Cas9-GFP/+; PER2::luc/+	Rosa26 knockin of LSL-Cas9-GFP driven by ubiquitous promoter. Cas9 and GFP were expressed in Aldh1L1(+) cells only. Global expression of PER2::luc.	AAV2/8-U6-sgBmal1-pCBh-mCherry^{NLS} (E1 or E3)	
Fig. S2				
sgLacZ	LSL-Cas9-GFP/+; PER2::luc/+	Rosa26 knockin of LSL-Cas9-GFP driven by ubiquitous promoter. Cas9 and GFP were expressed only in the presence of Cre recombinase. Global expression of PER2::luc.	AAV2/8-pCBh-Cre + AAV2/8-U6-sgLacZ-pCBh-mCherry^{NLS}	Ubiquitous expression of mCherry-NLS and Cre. Since lacZ is absence in the mammalian genome, sgLacZ is a control vector designed to test the specificity of sgRNA sequence.
sgBmal1 (E1 and E3)	LSL-Cas9-GFP/+; PER2::luc/+		AAV2/8-pCBh-Cre + AAV2/8-U6-sgBmal1-pCBh-mCherry^{NLS}	Ubiquitous expression of mCherry-NLS and Cre. In the presence of Cas9, a cut at a desired locus within

			(E1 or E3)	the Bmal1 gene was made and non-homologous end joining (NHEJ) of DNA leads to frame shift and premature stop codon in most Cas9-expressing cells.
Data not shown (related to fig. 3)				
AAV8-GFAP-GFP	Bmal1$^{f/f}$; PER2::luc/PER2::luc	Bmal1 conditional knockout in GFAP(+) cells. Global expression of PER2::luc.	AAV8-GFAP-GFP	GFP expression was driven by GFAP promoter.
AAV8-GFAP-Cre	Bmal1$^{f/f}$; PER2::luc/PER2::luc	Bmal1 conditional knockout. Global expression of PER2::luc.	AAV8-GFAP-Cre-GFP	Cre and GFP expression were driven by GFAP promoter.
Fig. 4a-d				
CK1ε$^{tau/+}$	CK1ε$^{tau/+}$; PER2::luc/+	Heterozygous *tau* mutation in casein kinase 1 epsilon gene led to short period (~22h) phenotype. Global expression of PER2::luc.	None.	None.
Aldh1L1-CK1ε$^{tau/+}$	Aldh1L1-Cre/+; CK1ε$^{tau/+}$; PER2::luc/+	Heterozygous *tau* mutation in casein kinase 1 epsilon gene led to short period (~22h) phenotype. The mutation was deleted in Aldh1L1(+) cells throughout the mouse, resulting in reversal of phenotype in those cells only. Global expression of PER2::luc.	None.	None.
Fig. 4e-j				
AAV8-	CK1ε$^{tau/+}$;	Heterozygous *tau* mutation in	AAV8-GFAP-GFP	GFP expression was driven

GFAP-GFP	PER2::luc/+	casein kinase 1 epsilon gene led to short period (~22h) phenotype. Global expression of PER2::luc.		by GFAP promoter.
AAV8-GFAP-Cre	$CK1\varepsilon^{tau/+}$; PER2::luc/+	Heterozygous *tau* mutation in casein kinase 1 epsilon gene led to short period (~22h) phenotype. The mutation was deleted in infected SCN GFAP(+) cells throughout the mouse, resulting in reversal of phenotype in those cells only. Global expression of PER2::luc.	AAV8-GFAP-Cre-GFP	Cre and GFP expression were driven by GFAP promoter.

Jackson Lab Stock Number or citation:

Aldh1L1-Cre/+	Jax: 023748
$CK1\varepsilon^{tau/tau}$	PMID: 18400165
LSL-Cas9-eGFP	Jax: 024858
$LSL\text{-}GFP^{NLS}$	Jax: 008516
PER2::luc	Jax: 006852
VIP-IRES-Cre	Jax: 010908
$Bmal1^{f/f}$	Jax: 007668

Supplemental Experimental Procedures

Immunohistochemistry.
Animals were sacrificed between ZT 2-4 by transcardial perfusion of PBS followed by 4% paraformaldehyde and their brains harvested and cryoprotected. We made 30 μm coronal brain sections using a cryostat. Immunostaining was performed as previously described. [S1] Primary antibodies used were rabbit anti-BMAL1 (NB100-2288, Novus, 1:5000), rabbit anti-GFAP (Z0334, Dako, 1:100), chicken anti-GFP (ab13970, Abcam, 1:2000), mouse anti-AVP (PS41, gift from Dr. Harold Gainer, NINDS, 1:50), and mouse anti-FOX2 (ab57154, Abcam, 1:200). Secondary antibodies used were Alexa Fluor 488-conjugated Goat anti-Chicken IgG, Cy3-conjugated Donkey anti-rabbit IgG, Alexa Fluor 594-conjugated Donkey anti-mouse IgG and Alexa Fluor 647-conjugated Donkey anti-rabbit IgG (all from Jackson Immuno Research, 1:500). Sections were mounted with ProLong® Gold Antifade Mountant with DAPI (Thermo Scientific). Images were acquired on a Nikon A1 confocal microscope as a single z-section (optical section thickness of 2.73μm). Images were taken sequentially averaging 4 images for each of the four-color channels. Observers blinded to the treatment groups counted cells within the SCN that expressed one or more of the targeted antigens using ImageJ software [S2].

Behavior recording.
Mice were maintained in the Danforth animal facility at Washington University. Adult mice were housed individually in cages equipped with running wheels and maintained in light-tight chambers illuminated with fluorescent bulbs (General Electric). Running wheel activity was recorded in 6-min bins (Clocklab, Actimetrics). Period was determined by χ^2 periodogram using Clocklab software.

Bioluminescence Recording.
Unless otherwise specified, 300-μm coronal SCN slices were prepared from adult animals. Briefly, mice were sacrificed with CO_2 and decapitated. Brains were quickly collected in chilled Hank's balanced salt solution (HBSS), pH 7.2 (Sigma), supplemented with 0.01 M HEPES (Sigma), 100 U/mL penicillin, 0.1 mg/mL streptomycin, and 4 mM $NaHCO_3$ (Invitrogen). Brain sections were obtained with a vibratome (OTS-5000; Electron Microscopy Sciences). Each SCN was dissected and cultured individually on a Millicell-CM membrane (Millipore) in a 35mm Petri dish with 1 mL of DMEM (Sigma) supplemented with 10 mM HEPES (Sigma), 2.2 mg/mL $NaHCO_3$ (Invitrogen), and 0.1 mM beetle D-luciferin (Biosynth). Petri dishes were sealed with vacuum grease and placed under photomultiplier tubes (HC135-11MOD; Hamamatsu) at 36 °C in the dark. Bioluminescence was recorded in 6-min bins (PER2::luc) or 10-min bins (AAV2/10-Bmal1ext-DIO-luc). Acquired *in vitro* bioluminescence traces were detrended by division and fitted with a damped sine function (Chronostar 1.0 [3]), and traces with a coefficient of correlation >0.80 and period between 18-30h were defined as circadian. The periods of PER2::luc and *Aldh1L1-Bmal1*^{luc} expression were determined using Chronostar software. For CCD recordings, *Aldh1L1-Bmal1*^{luc} SCN was imaged under 20x objective with 0.5x coupler using an ultrasensitive CCD camera (Andor iKon) mounted on an inverted microscope. Temperature was maintained at 35°C with a box incubator (In vivo Scientific). Static, cell-sized ROIs were drawn on the acquired movie in ImageJ and the acquired traces were processed through a custom Matlab script. Circadian traces from each movie were detrended by division and presented as a raster plot. We used Chronostar to determine period and rhythmicity from the raw traces. All ROIs that had a coefficient of correlation >0.80 and period between 18-30h were defined as circadian and the time of their second Bmal1-Luc peak was evaluated by a Rayleigh test of uniformity using the R package "circular". [S3]

Statistical Analysis.
All results were expressed as mean ± SEM. For comparisons of two groups of normally distributed data, Student's t-test was performed. One-way ANOVA with Sidak's multiple comparison test was used for data shown in Fig. 3e. GraphPad Prism 7 was used to perform statistical analysis and to generate figures.

Supplemental References

S1. An, S., Irwin, R.P., Allen, C.N., Tsai, C., and Herzog, E.D. (2011). Vasoactive intestinal polypeptide requires parallel changes in adenylate cyclase and phospholipase C to entrain circadian rhythms to a predictable phase. J Neurophysiol *105*, 2289-2296.

S2. Schneider, C.A., Rasband, W.S., and Eliceiri, K.W. (2012). NIH Image to ImageJ: 25 years of image analysis. Nat Methods *9*, 671-675.

S3. Maier, B., Wendt, S., Vanselow, J.T., Wallach, T., Reischl, S., Oehmke, S., Schlosser, A., and Kramer, A. (2009). A large-scale functional RNAi screen reveals a role for CK2 in the mammalian circadian clock. Genes Dev *23*, 708-718.